



Title	Long-term (2001-2012) observation of the modeled hygroscopic growth factor of remote marine TSP aerosols over the western North Pacific : impact of long-range transport of pollutants and their mixing states
Author(s)	Boreddy, S. K. R.; Kawamura, Kimitaka; Haque, Md. Mozammel
Citation	Physical chemistry chemical physics, 17(43), 29344-29353 https://doi.org/10.1039/c5cp05315c
Issue Date	2016-10-11
Doc URL	http://hdl.handle.net/2115/62997
Type	article (author version)
File Information	Final(4).pdf



[Instructions for use](#)



HOKKAIDO UNIVERSITY

Title	Long-term (2001-2012) observation of the modeled hygroscopic growth factor of remote marine TSP aerosols over the western North Pacific: impact of long-range transport of pollutants and their mixing states
Author(s)	Boreddy, S. K. R.; Kawamura, Kimitaka; Haque, Md. Mozammel
Citation	Physical chemistry chemical physics, 17(43): 29344-29353
Issue Date	2016-10-11
DOI	
Doc URL	http://hdl.handle.net/2115/62997
Right	
Type	article (author version)
Additional Information	
File Information	Final Manuscript- Revised-PCCP.pdf



[Instructions for use](#)

1 **Long-term (2001-2012) observation of the modeled hygroscopic growth**
2 **factor of remote marine TSP aerosols over the western North Pacific:**
3 **impact of long-range transport of pollutants and their mixing states**

4
5 S.K.R. Boreddy¹, Kimitaka Kawamura¹ and Md. Mozammel Haque^{1,2}
6

7 ¹Institute of Low Temperature Science, Hokkaido University, N19, W8, Kita-ku, Sapporo
8 060-0819, Japan.

9 ²Graduate School of Environmental Science, Hokkaido University, Sapporo, Japan.
10
11
12
13
14
15
16
17
18
19
20
21
22
23
24

25 *Corresponding author
26

27 Kimitaka Kawamura,
28 Institute of Low Temperature Science,
29 Hokkaido University,
30 Sapporo 060-0819, Japan.
31 E-mail:kawamura@lowtem.hokudai.ac.jp

Abstract

In order to assess the seasonal and annual variability of long-range transported anthropogenic pollutants from East Asia and their effect on the hygroscopicity and precipitation process over the western North Pacific, we conducted a long-term calculation of bulk hygroscopicity, $g(90\%)_{ZSR}$, based on ZSR model using chemical composition data during 2001-2012 at Chichijima Island. We found sea-salts (Na^+ and Cl^-) are the major mass fraction (65%) of total water-soluble matter followed by SO_4^{2-} (20%) and WSOM (6%). Seasonal variation of $g(90\%)_{ZSR}$ showed high in summer to autumn and low in winter to spring months, probably due to the influence of long-range transport of anthropogenic SO_4^{2-} , dust, and organics from East Asia and their interaction with sea-salts by heterogeneous reactions. On the other hand, annual variations of $g(90\%)_{ZSR}$ showed a decrease from 2001 to 2006 and then an increase from 2007 to 2012. Interestingly, the annual variations of SO_4^{2-} mass fractions showed an increase from 2001 to 2006 and then a decrease from 2007 to 2012, demonstrating that SO_4^{2-} seriously suppress the hygroscopic growth of sea-salt particles over the western North Pacific. This is further supported by the strong negative correlation between SO_4^{2-} and $g(90\%)_{ZSR}$. Based on the MODIS satellite data, the present study demonstrates that long-range transported anthropogenic pollutants from East Asia to the North Pacific can act as efficient cloud condensation nuclei but significantly suppress the precipitation by reducing the size of cloud droplet over the western North Pacific.

51

Keywords: Hygroscopicity, ZSR model, inorganic ions, organics, long-range transport, western North Pacific

54

55 1. Introduction

56 Particulate matter is microscopic solid or liquid suspended in the earth's atmosphere.
57 Although they represent a small portion of atmospheric mass, atmospheric particles largely
58 impact on climate and global biogeochemistry¹. Sea-salt particle is one of the most widely
59 distributed natural aerosols, which forms via the evaporation of sea-spray droplets produced
60 by the bubble bursting of entrained air during whitecap formation². They are characterized as
61 non-light-absorbing, highly hygroscopic, and coarse particles. Due to its strong hygroscopic
62 nature, a sea salt particle can serve as efficient cloud condensation nuclei (CCN), altering
63 cloud reflectivity, lifetime, and precipitation process³⁻⁵. Nonetheless, knowledge of
64 hygroscopicity of sea-salt aerosols and their impact on radiative forcing calculations are still
65 unclear⁶⁻⁷.

66 Atmospheric aerosols consist of organic and inorganic compounds with their internal
67 or external mixing. Hygroscopicity of aerosol particles is linked to the chemical composition
68 and their mixing states. Cruz and Pandis⁸ reported that organic acids such as glutaric and
69 pinonic acids generally increase the water uptake capability of $(\text{NH}_4)_2\text{SO}_4$ but decrease that
70 of NaCl salts based on a volume fraction relative to that of inorganic salts. Choi and Chan⁹
71 studied the effect of organic species (glycerol, succinic acid, malonic acid, citric acid, and
72 glutaric acid) on the hygroscopic behaviour of pure inorganic salts and found that the
73 presence of all these organics in the mixed particle reduces the water absorption of NaCl but
74 enhance that of $(\text{NH}_4)_2\text{SO}_4$ relative to that of the pure inorganic salts. Therefore, the
75 interaction between organic and inorganic species (or mixing state) in aerosol particles is
76 complex and this interaction acts either positively or negatively depending on the organic
77 mass fractions and salt types^{8, 10}.

78 Zdanovskii-Stokes-Robinson (ZSR) relation¹¹ is the most common model, used to
79 predict the hygroscopic growth of mixed aerosol particles using chemical composition data.
80 Sjogren et al.¹² reported that the measured hygroscopic growth factors at the high-alpine site,
81 Jungfraujoch, agreed well with predictions made by ZSR model. On the other hand, the
82 hygroscopicity of ambient marine aerosols show a significant underestimation compared to
83 the prediction estimated by numerical thermodynamic models¹³.

84 Anthropogenic emissions from East Asia have significantly increased over recent
85 decades due to the rapid growth of the East Asian economies, which are implausible to
86 decline in the next 20 years¹⁴. In addition, surface dust in spring is another distinct feature of
87 the air quality over East Asia and the outflow regions^{15, 16}. These anthropogenic pollutants
88 and dusts are transported from East Asia to the North Pacific by westerly winds^{17, 18} and

89 perturb the remote marine background conditions and modify the physico-chemical
90 properties of sea-salt particles as well as ocean biogeochemistry by heterogeneous reactions¹⁹.
91 However, there is still knowledge gap on how long-range transported anthropogenic
92 pollutants affect the precipitation process over the western North Pacific.

93 Chichijima Island is a remote marine site in the western North Pacific and is
94 geographically located in the outflow region of Asian dusts and anthropogenic pollutants
95 from East Asia during winter and spring, whereas pristine marine air masses dominate over
96 the island in summer and autumn²⁰. Therefore, this site is scientifically very important for
97 studying the long-range atmospheric transport of pollutants and mineral dusts and their
98 influence on the precipitation process; however, studies on long-term observations of
99 transported aerosols over the western North Pacific are limited^{20, 21}. Moreover, there is no
100 study on the long-term observation of hygroscopic growth factors from the western North
101 Pacific. In this study, we investigate seasonal and annual variation of the bulk hygroscopic
102 growth factor, $g(90\%)_{ZSR}$, derived from ZSR model. We also discuss the impact of long-
103 range atmospheric transport of anthropogenic pollutants and their mixing states on marine
104 bulk hygroscopicity and precipitation process over the western North Pacific during the study
105 period of 2001-2012.

106 The hygroscopic growth of fine and coarse particles should have different pictures
107 because of different chemical compositions and sizes, thus, their atmospheric importance is
108 dissimilar. Fine size particles are important for CCN formation, while coarse particles are
109 playing a major role on the radiative impacts of aerosol particles. However, physico-chemical
110 processes (coagulation and condensation as well as heterogeneous reactions) could make fine
111 particles to be larger particles in the water mediated atmosphere (under high RH conditions).
112 As a result, background conditions of the atmosphere may perturb, especially over the marine
113 atmosphere. In the present study, the estimated hygroscopic growth factors from TSP
114 aerosols would better elucidate about the mixing state of the above mentioned aerosol
115 particles and their climatic effects.

116 **2. Methods**

117 **2.1. Aerosol sampling**

118 Aerosol (TSP) samples were collected on pre-combusted (450 °C, 3 hours) quartz
119 filter (20 x 25 cm, Pallflex 2500QAT-UP) at 5 m above the ground level of Satellite Tracking
120 Centre of Japan Aerospace Exploration Agency (JAXA, elevation 254 m) in Chichijima
121 Island (27°04' N; 142°13' E) using a high volume air sampler with a flow rate of 1 m³ min⁻¹
122 during 2001-2012²⁰. Aerosol samples were collected on a weekly basis, because of less local

123 pollution at Chichijima Island. After sampling, filters were put in a clean glass jar with a
 124 Teflon-lined screw cap and stored at -20 °C.

125 **2.2. Analysis of Chemical species**

126 For water-soluble inorganic species, a filter cut of 20 mm in diameter from each filter
 127 was extracted with 10 mL of organic-free ultra pure water (>18.2 MΩcm) under
 128 ultrasonication and filtrated through disk filters (Millex-GV, 0.22 μm, Millipore). These
 129 filtrated extracts were analyzed for inorganic species using an ion chromatography (761
 130 Compact IC, Metrohm) and results were reported in elsewhere (Boreddy and Kawamura,
 131 2015). For water-soluble organic carbon (WSOC), a punch of 20 mm was extracted with 20
 132 mL of organic-free ultra pure water under ultrasonication and filtrated through a disk filters
 133 (Millex-GV, 0.22 μm, Millipore). These extracts were analyzed for WSOC using Total
 134 Carbon Analyzer (TOC-Vcsh, Shimadzu, Japan)²².

135 **2.3. The ZSR relation**

136 The Zdanovskii-Stokes-Robinson (ZSR) model¹¹, which relates the hygroscopicity of
 137 mixture to that of the individual components at the same relative humidity (RH). The
 138 hygroscopic growth factor of aerosol particle can be predicted from the growth factors of
 139 individual components of the aerosol composition and their respective volume fractions (ε)
 140 using ZSR relation as,

$$141 \quad g(RH)_{ZSR} = \left(\sum_i \varepsilon_i g_i(RH)^3 \right)^{\frac{1}{3}} \quad (1)$$

142 where $g(RH)_{ZSR}$ is the growth factor of the mixed particle, $g_i(RH)$ and ε_i are the growth factor
 143 of individual component and their respective volume fraction, respectively. The volume
 144 fractions are calculated by assuming that the dry aerosol is composed of sodium chloride,
 145 ammonium sulfate, ammonium chloride, sodium nitrate, sodium sulfate and water-soluble
 146 organic matter. Rest of the volume fractions is neglected because of its low abundance to
 147 WSM.

148 The ZSR model assumes that the particles are spherical and their mixing behaviour is
 149 ideal and also hygroscopic growth of the organic and inorganic components is independent.

150 **3. Results and discussion**

151 **3.1 Validation of bulk $g(90\%)_{ZSR}$**

152 In order to validate the retrieved growth factor, $g(90\%)_{ZSR}$, of TSP aerosols obtained
 153 from ZSR model, we compared $g(90\%)_{ZSR}$ with measured growth factor, $g(90\%)_{HTDMA}$, using
 154 HTDMA during 2001-2003 over the same sampling site⁷ as shown in Fig. 1. We found that
 155 $g(90\%)_{ZSR}$ are strongly correlated with $g(90\%)_{HTDMA}$ with a correlation coefficient (R^2) of

156 0.80 and this correlation is statistically significant at the 99% confidence level (probability
157 value less than 0.001). It can be seen from Fig. 1 that the difference in standard deviation
158 (standard error) between the $g(90\%)_{ZSR}$ and $g(90\%)_{HTDMA}$ is 0.04 (0.006). We also found that
159 $g(90\%)_{ZSR}$ are overestimated by on average 15%, probably due to the presence of marine
160 organic compounds and the subsequent formation of less hygroscopic organic salts through
161 aqueous phase reactions⁷. As a result, $g(90\%)_{HTDMA}$ may be decreased due to the internal
162 mixing of chemical species and subsequent formation of less water-soluble salts.

163 Interestingly, this discrepancy in growth factor showed higher in spring followed by
164 winter and lowest in summer, indicating that interactions of water-soluble organics with dust
165 particles (for example, formation of CaC_2O_4) can suppress the hygroscopic growth of
166 particles in the outflow regions of Asian dust in spring. This point will be discussed more in
167 the following section 3.4. This is further supported by the previous studies^{7, 13, 23-26}, which
168 reported that ambient marine aerosol particles with less than 30% organic mass show a 15%
169 decrease in the hygroscopic growth factor. This perturbation adds significant uncertainty to
170 the radiative balance calculations. However, in the present study, we found that contribution
171 of WSOM to total water-soluble matter (WSM) is less than 30% (on average 6%). Therefore,
172 it is reasonable to use ZSR model to predict the hygroscopic growth factors over the western
173 North Pacific.

174 **3.2. Temporal and seasonal trends in major mass fractions of WSM and $g(90\%)_{ZSR}$**

175 Fig. 2 presents the temporal variation of major chemical mass fractions (Cl^- , Na^+ ,
176 SO_4^{2-} , NO_3^- and WSOM) of WSM and the $g(90\%)_{ZSR}$ of TSP aerosols collected at Chichijima
177 Island in the western North Pacific during 2001-2012. Sea-salt components (i.e., Na^+ and Cl^-)
178 are found to compose a major mass fraction (range: 0.00-0.88 and 0.03-0.41, respectively),
179 whose abundances are on average more than three times higher than SO_4^{2-} (0.00-0.77), ten
180 times higher than WSOM (0.00-0.57), and sixteen times higher than NO_3^- (0.00-0.14) mass
181 fractions. The $g(90\%)_{ZSR}$ values ranged from 1.63 to 2.28 with an average of 2.07 ± 0.09
182 during the study period of 2001-2012. Although there is no clear increasing or decreasing
183 temporal trends in all the species during the study period, a similar variation can be seen
184 between the $g(90\%)_{ZSR}$ and sea-salt components, indicating that the hygroscopicity of
185 Chichijima aerosols is mainly controlled by sea salt particles.

186 Interestingly, anti-correlations were found between the $g(90\%)_{ZSR}$ and WSOM, SO_4^{2-} ,
187 and NO_3^- . These results indicate that anthropogenic pollutants, water-soluble organic matter
188 and their mixing state can alter the hygroscopicity of sea-salt particles through the

189 heterogeneous reactions, in particular, during the period of continental outflow over the
190 western North Pacific. These points will be discussed in more detail in the following sections.

191 The seasonal variations in $g(90\%)_{ZSR}$ and major chemical mass fractions of total
192 WSM are shown in Fig. 3a-f during 2001-2012. The vertical hinges represent data points
193 from lower to upper quartile (i.e., 25th and 75th percentiles). The whiskers represent data
194 points from the 5th to 95th percentiles. We found a clear seasonal variation in all the
195 chemical mass fractions, which are clearly reflected in the $g(90\%)_{ZSR}$. These seasonal
196 differences are verified by *t*-test. These results show that these differences are statistically
197 significant with two tailed *p* values of less than 0.001. As illustrated in Fig. 3a, monthly
198 means of $g(90\%)_{ZSR}$ are high in autumn followed by summer and scarce in spring and winter
199 months, probably due to the atmospheric processing associated with dechlorination that may
200 decrease the growth factor over the western North Pacific, especially during the period of
201 continental outflow.

202 It is noteworthy that the similar seasonal pattern can be seen in the mass fractions of
203 sea-salt particles (see Fig. 3b and c). On the other hand, SO_4^{2-} and NO_3^- mass fractions are
204 maximized in spring followed by winter, probably due to the long-range atmospheric
205 transport of anthropogenic pollutants from East Asia and minimized in summer and autumn
206 months (see Fig. 3d and e). Mass fractions of WSOM are higher in summer followed by
207 spring and lower in autumn (see Fig. 3f). We again found an opposite trend between the mass
208 fractions of Cl^- and SO_4^{2-} and similar trend between the $g(90\%)$ and Cl^- mass fraction,
209 demonstrating that SO_4^{2-} seriously suppresses the hygroscopic growth of sea-salt particles
210 along with WSOM via heterogeneous reactions over the western North Pacific. This point
211 will be discussed in more details in the following sections.

212 3.3. Annual trends in major mass fractions of WSM and $g(90\%)_{ZSR}$

213 Fig. 4a-d presents the annual variation of $g(90\%)_{ZSR}$ and mass fractions of selected
214 components for different seasons during the period of 2001-2012. It can be clearly seen from
215 Fig. 4a that $g(90\%)_{ZSR}$ showed a clear annual trend with a decrease from 2001 to 2006 and
216 then an increase from 2007 to 2012 in winter and autumn. In spring, we couldn't find any
217 clear annual trend, probably due to the influence of organo-metallic interaction during long-
218 range transport of Asian dusts⁷. On the other hand, the annual variation of mass fractions of
219 SO_4^{2-} showed an increase from 2001 to 2006 and a decrease from 2007-2012 ($p < 0.005$). Lu et
220 al.²⁷ reported that the emission rate of SO_2 over East Asia slowed down around 2005 and
221 began to decrease after 2006. The reduction in SO_2 emissions in China was mainly due to the
222 wide usage of Flue-Gas Desulfurization (FGD) devices in power plants. Similar annual

223 pattern can also be seen in the mass fractions of NO_3^- . Mass fractions of WSOM showed a
224 clear annual trend ($p < 0.005$) in winter with an increase from 2001 to 2006 and a decrease
225 from 2007-2012 (see Fig. 4d). Based on all these results, we demonstrate that although
226 WSOM often acts to decrease the hygroscopicity over the western North Pacific,
227 anthropogenic SO_4^{2-} and NO_3^- that are long-range transported from East Asia also suppress
228 the hygroscopic growth of sea-salt particles during winter and spring months.

229 **3.4. A relation between $g(90\%)_{\text{ZSR}}$ and chemical mass fractions of WSM**

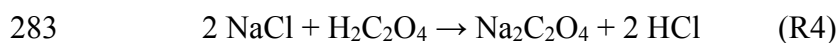
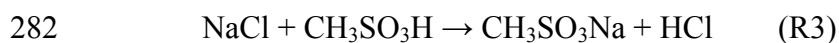
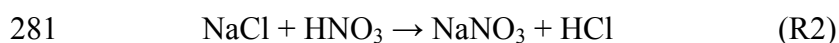
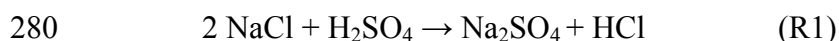
230 Chemical compositions and their mixing states are crucial for modelling studies on
231 the hygroscopic²⁸ and optical properties²⁹ of aerosol particles, which provide the information
232 about their chemical aging³⁰. Fig. 5 shows the scatter plots between the $g(90\%)_{\text{ZSR}}$ and mass
233 fractions of different chemical species and/or components for different seasons during 2001-
234 2012. Their corresponding Pearson correlation coefficient (R) values are reported in Table 1.
235 We found an excellent positive correlation (range: 0.87 to 0.92) between Cl^- mass fractions
236 and $g(90\%)_{\text{ZSR}}$ for all seasons, demonstrating that the growth factors at Chichijima Island are
237 mainly controlled by sea-salt particles as shown in Fig. 5a. Mass fractions of Mg^{2+} show
238 good correlations with $g(90\%)_{\text{ZSR}}$ in winter (0.56), followed by summer (0.44) and spring
239 (0.34), but weakly correlated in autumn (0.18) (Fig. 5h). These results indicate that Mg^{2+}
240 also can partially contribute to the hygroscopicity because Mg^{2+} largely comes from the
241 ocean rather than continental sources²⁰. We also found a strong positive correlation (0.73 to
242 0.86) between Cl^-/Na^+ mass fraction ratio and $g(90\%)_{\text{ZSR}}$ in all seasons (see Fig. 5j). These
243 results demonstrate that the hygroscopicity at Chichijima Island is mainly controlled by the
244 sea-salt particles and atmospheric processing associated with chloride depletion that may
245 suppress the hygroscopic growth of marine aerosol particles.

246 In contrast, SO_4^{2-} and WSOM showed strong negative correlations (-0.70 to -0.90 and
247 -0.6 to 0.82) with $g(90\%)_{\text{ZSR}}$, especially during the period with an influence of continental
248 outflow from East Asia (winter and spring). On the other hand, mass fractions of NH_4^+ and
249 NO_3^- also negatively correlated with $g(90\%)_{\text{ZSR}}$. These results demonstrate that mixing of
250 anthropogenic pollutants (such as SO_2 and NO_x) with inorganic or organic species that can
251 convert the high hygroscopic salts (NaCl) into low hygroscopic salts ($(\text{NH}_4)_2\text{SO}_4$, Na_2SO_4 ,
252 NaNO_3 , etc.) by heterogeneous reactions (see reactions R1 to R6) and other physical
253 mechanisms such as coagulation and condensation during long-range atmospheric transport.
254 Moreover, in spring, Asian dusts can interact with organics and leads to the formation of less
255 hygroscopic salts such as calcium oxalate⁷ or ammonium oxalate.

256 This is further supported by the negative correlation (0.25) between $g(90\%)_{ZSR}$ and
 257 Ca^{2+} during the spring. We also found good correlation between NH_4^+ and oxalic acid during
 258 winter ($R=0.75$; $p<0.0001$) and spring ($R=0.54$; $p<0.001$), suggesting the formation of
 259 ammonium oxalate over the western North Pacific. This correlation is more significant in
 260 winter than spring, probably due to the long-range atmospheric transport of biomass burning
 261 aerosols from East Asia. Reid et al.^{31, 32} documented that NH_4^+ was significantly correlated
 262 with organic species, such as oxalic acid rather than SO_4^{2-} in the regional haze dominated by
 263 biomass burning smoke in Brazil. Our recent study³⁰ also supported the formation of
 264 ammonium oxalate in biomass burning aerosols collected at Tanzania, East Africa. Hence, it
 265 is likely that biomass burning may be a significant source of formation of ammonium oxalate.
 266 This result is further supported by significant negative correlations between $g(90\%)_{ZSR}$ and
 267 oxalic acid during winter (-0.63) and spring (-0.43) (see Table 1).

268 Ma and He³³ reported that formation of calcium nitrate will also lower the
 269 hygroscopicity of particles by mixing with oxalic acid (see reaction R6). The internal mixing
 270 of oxalic acid with sea-salt particles also leads to lower the hygroscopicity during the long-
 271 range atmospheric transport³⁴. This kind of mixing in the dust particles is very important for
 272 explaining the mass transfer process in the atmosphere³⁵ and direct and indirect climate
 273 forcing of dust particles^{36, 37}. Therefore, it is important to note that the declined $g(90\%)_{ZSR}$ in
 274 winter and spring was probably due to the formation of less hygroscopic particles or salts
 275 through heterogeneous reactions that play a significant role in aged mineral dust particles and
 276 anthropogenic pollutants, resulting in a decrease of the hygroscopic growth of marine aerosol
 277 particles. The possible acid displacement reactions, which occur over the western North
 278 Pacific, are given below.

279



286

287 Previous studies have shown that more hygroscopic group of particles is often
 288 observed in remote marine environment⁶. Growth factors of this group ($g(90\%)>1.85$) are
 289 larger than those of pure ammonium sulfate ($g(90\%)=1.70$) and pure ammonium bisulphate

290 (g(90%)=1.79). During the strong influence of continental outflow of air masses, an uptake of
291 H_2SO_4 (or HNO_3) by sea-salt particles followed by the subsequent release of HCl, for
292 example, converts some of NaCl (g(90%)=2.4) into sodium sulfate (g(90%)<1.8) (or sodium
293 nitrate) by the above mentioned reactions (R1 or R2). The formation of sodium sulfate (or
294 sodium nitrate) will result in a significant reduction in the growth factor of sea-salt particles
295 and thus affect the CCN and precipitation process over the western North Pacific.

296 Fig. 6 presents the schematic diagram, which shows the changes in microphysical and
297 chemical properties of sea-salt particles under the influence of two distinct air masses that
298 aged over the western North Pacific. The observation site, Chichijima, is a remote Island in
299 the western North Pacific located in the outflow region of Asian dust and anthropogenic
300 pollutants from East Asia, especially from China. This sampling site exists in the boundary of
301 the westerly (in winter and spring) and easterly (in summer and autumn) wind regimes.

302 During the long-range atmospheric transport of air masses by westerly winds, sea-salt
303 particles are seriously modified by internal mixing of anthropogenic pollutants and dust
304 particles through heterogeneous reactions as mentioned above (R1-R6). This mixing state,
305 together with long-range transport of pollutants from East Asia, can depress the water uptake
306 properties of sea-salts due to the formation of less hygroscopic particles and can increase the
307 number of smaller size CCN particles, leading to the formation of smaller size of cloud
308 droplets, an enhanced reflection of solar radiation (less transmission), and an increase in
309 cloud lifetime. Moreover, smaller size particles absorb more radiation and suppress the
310 precipitation process by cloud evaporation or simply cloud burning.

311 On the other hand, easterly (trade) winds with low wind speed carry pristine air
312 masses to the sampling site especially in summer and autumn (see Fig. 6). In this process,
313 sea-salt particles uptake more water acting as giant CCNs, which could be nucleated into
314 larger cloud particles. By coagulation and condensation, less absorptive and more transmittant
315 cloud particles grow into rain droplets hence enhancing precipitation process. Although the
316 present study focus on the hygroscopic growth factor of bulk aerosols, the implications of
317 these results (such as a reduction in water uptake of sea-salt particles due to internal mixing
318 of sulfate/nitrate particles and organics) directly affect the CCN number concentrations by
319 decreasing the size of particles and hence increases the number of smaller sized particles due
320 to the continental influence (see Fig.6). However, measurements of particle number size
321 distributions are required to further confirm these results.

322 These results are further supported by the MODIS aqua satellite
323 (<http://gdata1.sci.gsfc.nasa.gov>) products and precipitation (downloaded from

324 <http://www.jma.go.jp>) at Chichijima Island in the western North Pacific during 2001-2012.
325 Figs. 7a-b illustrate the seasonal variations of $g(90\%)_{ZSR}$ and precipitation at Chichijima
326 Island during 2001-2012. The precipitations at Chichijima clearly increased from winter to
327 autumn with lower precipitation values during westerly and higher values in trade wind
328 regimes. Fascinatingly, we found similar seasonal trend in $g(90\%)_{ZSR}$, although we found a
329 significant reduction in the growth factors during spring, which may be due to the influence
330 of Asian dusts. These results demonstrate that westerly winds transported anthropogenic
331 pollutants that suppress the hygroscopicity as well as precipitation over the western North
332 Pacific by enhancing the CCN, COD (Cloud Optical Depth, a proxy for cloud cover) and
333 other aerosol products, such as AOD (Aerosol Optical Depth at 550 nm, a proxy for fine
334 mode aerosols), and particulate organic carbon concentrations, as shown in Figs. 7c-f,
335 respectively. All the satellite-derived products are abundant during winter and spring
336 (westerly) whereas scarce in summer and autumn (trade wind).

337 We also found a good opposite seasonal trend between the modeled $g(90\%)_{ZSR}$ and
338 particulate organic carbon concentrations, indicating that organics in aerosols suppress the
339 hygroscopic growth over the western North Pacific. Further, a robust opposite seasonal
340 variation was found between precipitation and particulate organic carbon concentrations,
341 demonstrating that particulate organics repress the precipitation by boosting up the CCN
342 concentrations. Based on the above-mentioned results, it is reasonable to conclude that the
343 long-range atmospheric transport of pollutants from East Asia are significantly enhancing the
344 fine size CCN concentration, but seriously suppress the hygroscopic growth of aerosols
345 affecting the precipitation over the western North Pacific.

346 Previous studies suggested that polluted aerosols suppress deep convective
347 precipitation by decreasing cloud droplet size and delaying the onset of freezing³⁸⁻⁴⁰. In the
348 modeling study by Cui et al.⁴¹, the less precipitation is caused by drops evaporating more
349 rapidly in the high aerosol case⁴², which eventually reduces ice mass and hence precipitation.
350 In contrast, Koren et al.⁴³ found, based on satellite data analyses, that increases in aerosol
351 abundance correlated with a higher rate of rainfall in the tropics, subtropics and mid-latitudes.
352 They also mentioned that the similar trends were seen across different locations and
353 environmental conditions, suggesting a link between increased aerosol levels and more
354 intense rainfall. However, their observation period is limited to specific season (June-August
355 2007) and they didn't discuss the effect of long-range transport of pollutants and their relation
356 to precipitation. The present study should contribute to clarifying the above uncertainty, that

357 is, anthropogenic chemical species in the midlatitudes can depress the rainfall intensity in the
358 open ocean.

359 Therefore, the above results highlight the complexity of the aerosol-cloud-
360 precipitation system and demonstrate the sign for the global change in precipitation due to
361 changes in the concentrations and composition of aerosols. It is important to note that
362 microphysical processes can only change the temporal and spatial distribution of precipitation
363 while the total amount of precipitation can only change if evaporation from the surface
364 changes.

365 **3.5 Atmospheric implication and conclusions**

366 The purpose of this study has been to observe the long-term (2001-2012) variations in
367 hygroscopic properties of TSP aerosols and their relation to the precipitation over the western
368 North Pacific. We found the bulk hygroscopicity of remote marine aerosols is mainly
369 controlled by sea-salt particles (NaCl) because of its high abundances in total WSM.
370 However, anthropogenic pollutants that are transported from East Asia are internally mixed
371 with sea-salt particles by heterogeneous reactions, leading to a suppression of the
372 hygroscopic growth thus affecting the CCN properties especially during winter and spring.
373 On the other hand, WSOM may often suppress the hygroscopic growth of remote marine
374 aerosols over the western North Pacific. We also found that there is a serious impact of Asian
375 dust and their interactions with organic/inorganic salts on hygroscopic growth.

376 Although there is no clear decadal trend in $g(90\%)_{ZSR}$, we found a systematic seasonal
377 variation with high values in autumn and summer and low values in spring and winter. In
378 winter and autumn, the annual variation of $g(90\%)_{ZSR}$ decreased from 2001 to 2007 and then
379 increased continuously toward 2012. At the same time, SO_4^{2-} mass fractions increased from
380 2001 to 2006 and then decreased to 2012 probably due to the decrease in SO_2 emissions in
381 China after 2006. These results demonstrate that anthropogenic sulfate seriously suppress the
382 hygroscopic growth of marine aerosol particles through heterogeneous reactions over the
383 western North Pacific, especially during long-range atmospheric transport. This is further
384 supported by the regression analyses between $g(90\%)_{ZSR}$ and mass fractions of WSM during
385 the study period. The present study also demonstrates that long-range atmospheric transport
386 of pollutants from East Asia can enhance the CCN activity but suppress the precipitation by
387 reducing the droplet size over the western North Pacific. However, size-segregated
388 measurements may provide a different picture of hygroscopic properties, depending on the
389 particle size, for variable chemical compositions.

390 In this study, we found that these modified sea salts have profound consequences on
391 their evolving physicochemical properties especially on hygroscopic behaviour by increasing
392 cloud droplet number concentration and reducing the cloud droplet size and thus reducing
393 precipitation process. Therefore, in the marine atmosphere, the above consequences should
394 add significant uncertainty to the climatic and radiative models.

395 **Acknowledgements**

396 This study was in part supported by the Japan Society for the Promotion of Science (JSPS)
397 through grant-in-aid 1920405 and 24221001. We appreciate the financial support of a JSPS
398 fellowship to S. K. R. Boreddy. The MODIS data used in this study were acquired as part of
399 NASA's Earth Science Enterprise. The authors wish to thank the data distribution centres for
400 their support.

401

402 **References**

- 403
- 404 1. N. Mahowald et al., *Annu Rev Env Resour.*, 2011, 36, 45-74.
- 405 2. D. C. Blanchard, *J. Geophys. Res.: Oceans*, 1985, 90, 961-963.
- 406 3. T. Ayash, S. Gong, and C. Q. Jia, *J. Climat.*, 2008, 21, 3207-3220.
- 407 4. D. Rosenfeld, U. Lohmann, C. D. O'Dowd, M. Kulmala, S. Fuzzi, A. Reissell, and M.
- 408 O. Andreae, *Sci.*, 2008, 321 (5894), 1309-1313.
- 409 5. C. D. O'Dowd, J. A. Lowe, and M. H. Smith, *Atmos. Environ.*, 1999, 33, 3053-3062.
- 410 6. M. Mochida et al., *J. Geophys. Res.-Atmos.*, 2011, 116, doi:10.1029/2010jd014759.
- 411 7. S. K. R. Boreddy, K. Kawamura, and J. S. Jung, *J. Geophys. Res.-Atmos.*, 2014, 119,
- 412 167-178.
- 413 8. C. N. Cruz and S. N. Pandis, *Environ. Sci. Technol.*, 34, 2000, 4313-4319.
- 414 9. M. Y. Choi and C. K. Chan, *Environ. Sci. Technol.*, 2002, 36 (11), 2422-2428.
- 415 10. Z. J. Wu, A. Nowak, L. Poulain, H. Herrmann, and A. Wiedensohler, *Atmos. Chem.*
- 416 *Phys.*, 2011, 11, 12617-12626.
- 417 11. R. H. Stokes, and R. A. Robinson, *J. Phys. Chem.* 1966, 70, 2126-2131.
- 418 12. S. Sjogren et al., *Atmos. Chem. Phys.*, 2008, 8, 5715-5729.
- 419 13. Y. Ming, and L. M. Russell, *J. Geophys. Res.: Atmos.*, 2001, 106, 28259-28274.
- 420 14. Y. Zhao, J. Zhang, and C. P. Nielsen, *Atmos. Chem. Phys.*, 2014, 14, 8849-8868.
- 421 15. J. Sun, M. Zhang and T. Liu, *J. Geophys. Res.: Atmos.* 2001, 106, 10325-10333.
- 422 16. G. Wang, C. Cheng, J. Meng, Y. Huang, J. Li, and Y. Ren, *Atmos. Environ.*, 2015,
- 423 113, 169-176.
- 424 17. K. Kawamura, Y. Ishimura, and K. Yamazaki, *Global Biogeochem. Cycles* 2003, 17,
- 425 1003, doi:10.1029/2001GB001810.
- 426 18. K. Matsumoto, Y. Uyama, T. Hayano, and M. Uematsu, *J. Geophys. Res.: Atmos.*
- 427 2004, 109, D21206..
- 428 19. Y. Rudich, O. Khersonsky, and D. Rosenfeld, *Geophys. Res. Lett.* 2002, 29, 2064.
- 429 20. S. K. R. Boreddy, and K. Kawamura, *Atmos. Chem. Phys.* 2015, 15, 6437-6453.
- 430 21. S. K. Verma, K. Kawamura, J. Chen, P. Fu, and C. Zhu, *J. Geophys. Res.: Atmos.*
- 431 2015, 120, 4155-4168.
- 432 22. Y. Miyazaki, K. Kawamura, J. Jung, H. Furutani, and M. Uematsu, *Atmos. Chem.*
- 433 *Phys.* 2011, 11, 3037-3049.
- 434 23. O.H. Berg, K. Hämeri, E. Swietlicki, J. Zhou, M. Väkevä, and J. M. Mäkelä, *J. Aero.*
- 435 *Sci.*, 1998, 29, Supplement 2, S1101-S1102.
- 436 24. K. C. Kaku et al., *Atmos. Chem. Phys.* 2006, 6, 4101-4115.
- 437 25. E. Swietlicki et al., *Tellus B* 52, 2000, 201-227.
- 438 26. J. Zhou, et al., *J. Geophys. Res.- Atmos.*, 2001, 106, 32111-32123.
- 439 27. Z. Lu et al., *Atmos. Chem. Phys.* 2010, 10, 6311-6331.
- 440 28. K. Okada et al., *Atmos. Environ.*, 2005, 39, 5079-5089.
- 441 29. M. Pósfai, J. R. Anderson, P. R. Buseck, and H. Sievering, *J. Geophys. Res.: Atmos.*,
- 442 1999, 104, 21685-21693.
- 443 30. S. K. R. Boreddy, K. Kawamura, S. Mkoma, and P. Fu, *J. Geophys. Res.: Atmos.*,
- 444 2014, 119, 12233-12245.
- 445 31. J. S. Reid, P. V. Hobbs, R. J. Ferek, D. R. Black, J. V. Martines, M. R. Dunlap, and C.
- 446 Lioussé, *J. Geophys. Res.*, 1998, 103(D24), 32,059-32,080.
- 447 32. J. S. Reid, R. Koppmann, T. F. Eck, and D. P. Eleuterio, *Atmos. Chem. Phys.*, 2005, 5,
- 448 799-825.
- 449 33. Q. Ma, and H. He, *Atmos. Environ.* 2012, 50, 97-102.
- 450 34. Q. Ma, H. He, and C. Liu, *Atmos. Environ.* 2013, 69, 281-288.

- 451 35. V. A. Karydis, A. P. Tsimpidi, W. Lei, L. T. Molina, and S. N. Pandis, *Atmos. Chem.*
452 *Phys.* 2011, 11, 13305-13323.
- 453 36. R. C. Sullivan, S. A. Guazzotti, D. A. Sodeman, Y. Tang, G. R. Carmichael, and K. A.
454 Prather, *Atmos. Environ.* 2007, 41, 7166-7179.
- 455 37. R. C. Sullivan, M. J. K. Moore, M. D. Petters, S. M. Kreidenweis, G. C. Roberts, and
456 K. A. Prather, *Phys. Chem. Chem. Phys.* 2009, 11, 7826-7837.
- 457 38. D. Rosenfeld, *Geophys. Res. Lett.*, 1999, 26, 3105–3108.
- 458 39. D. Rosenfeld, and W. L. Woodley, *Nature*, 2000, 405, 440–442.
- 459 40. A. P. Khain, D. Rosenfeld, and A. Pokrovsky, *Geophys. Res. Lett.*, 2001, 28, 3887-
460 3890.
- 461 41. Z. Q. Cui, K. S. Carslaw, Y. Yin, and S. Davies, *J. Geophys. Res.*, 2006, 111,
462 doi:10.1029/2005JD005981, d05201.
- 463 42. H. L. Jiang, H. W. Xue, A. Teller, G. Feingold, and Z. Levin, *Geophys. Res. Lett.*,
464 2006, 33, doi:10.1029/2006GL026024,114806.
- 465 43. I. Koren, O. Altaratz, L. A. Remer, G. Feingold, J. V. Martins, and R. H. Heiblum,
466 *Nature Geosci.*, 2012, 5, 118-122.
- 467
468
469
470
471
472
473
474
475
476
477
478
479
480
481
482
483
484
485
486
487
488
489
490
491
492
493
494
495
496
497
498
499
500

501 **Table 1.** Pearson correlation coefficient (R) values between $g(90\%)_{ZSR}$ and chemical mass
 502 fractions for different seasons during 2001-2012 at Chichijima Island over the western North
 503 Pacific.

504
505
506

Species	$g(90\%)_{ZSR}$			
	Winter (n=132)	Spring (n=138)	Summer (n=132)	Autumn (n=143)
Cl ⁻	0.92 [*]	0.90 [*]	0.87 [*]	0.88 [*]
NO ₃ ⁻	-0.58 [*]	-0.41 [*]	-0.34 [*]	-0.51 [*]
SO ₄ ²⁻	-0.88 [*]	-0.82 [*]	-0.70 [*]	-0.90 [*]
Na ⁺	0.77 [*]	0.74 [*]	0.70 [*]	0.66 [*]
NH ₄ ⁺	-0.7 [*]	-0.71 [*]	-0.58 [*]	-0.57 [*]
K ⁺	-0.49 [*]	-0.33 [*]	-0.39 [*]	-0.44 [*]
Ca ²⁺	-0.15 [#]	-0.25 [#]	-0.19 [#]	-0.23 [#]
Mg ²⁺	0.56 [*]	0.34 [*]	0.44 [*]	0.18 [#]
WSOM	-0.82 [*]	-0.60 [*]	-0.67 [*]	-0.53 [*]
Oxalic acid	-0.64 [*]	-0.43 [*]	-0.39 [*]	-0.57 [*]
Cl ⁻ /Na ⁺	0.86 [*]	0.73 [*]	0.77 [*]	0.78 [*]

507 ^{*}Correlation is significant at less than 0.001 levels (2-tailed)

508 [#]Correlation is significant at 0.05 levels (2-tailed)

509
510
511
512
513
514
515
516
517
518
519
520
521
522
523
524
525
526
527
528
529
530
531
532
533
534
535
536

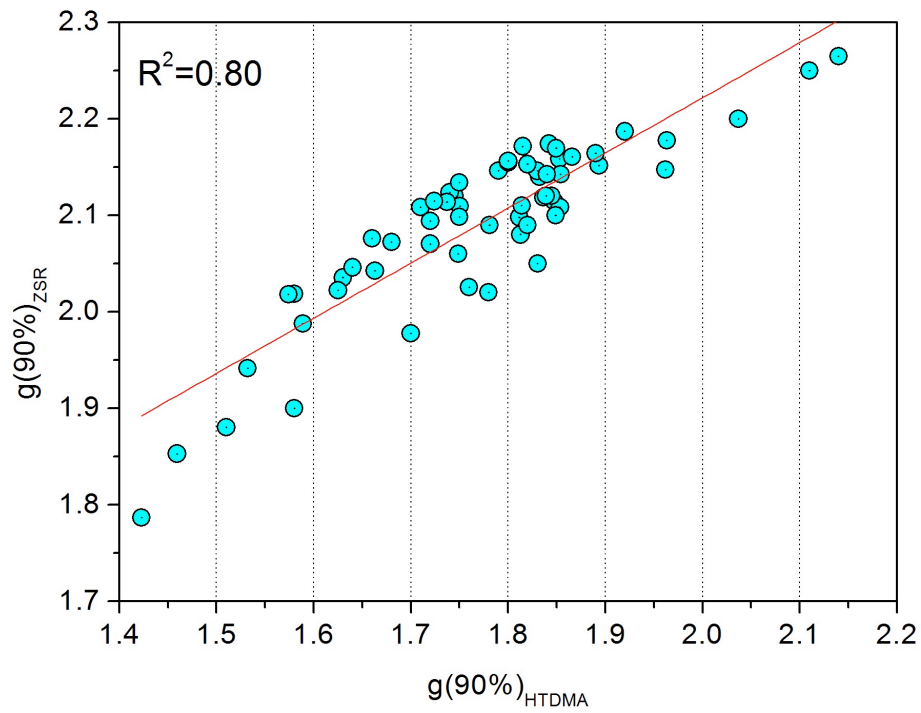


Fig. 1. Validation of modeled $g(90\%)_{ZSR}$ with measured $g(90\%)_{HTDMA}$ at Chichijima Island in the western North Pacific during 2001-2003.

563
 564
 565
 566
 567
 568
 569
 570
 571
 572
 573
 574
 575
 576
 577
 578
 579
 580
 581
 582
 583
 584
 585
 586
 587
 588
 589

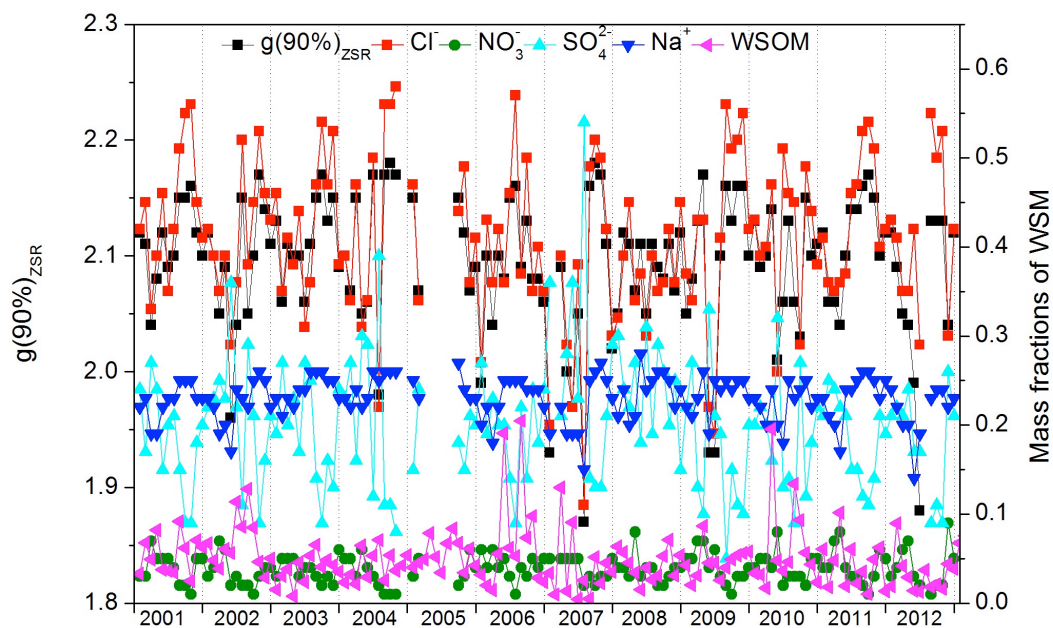


Fig. 2. Temporal variations in the $g(90\%)_{ZSR}$ and mass fractions of water-soluble matter at Chichijima Island in the western North Pacific during 2001-2012. Mass fractions are calculated using the data of ions and WSOC are taken from Boreddy and Kawamura (2015).

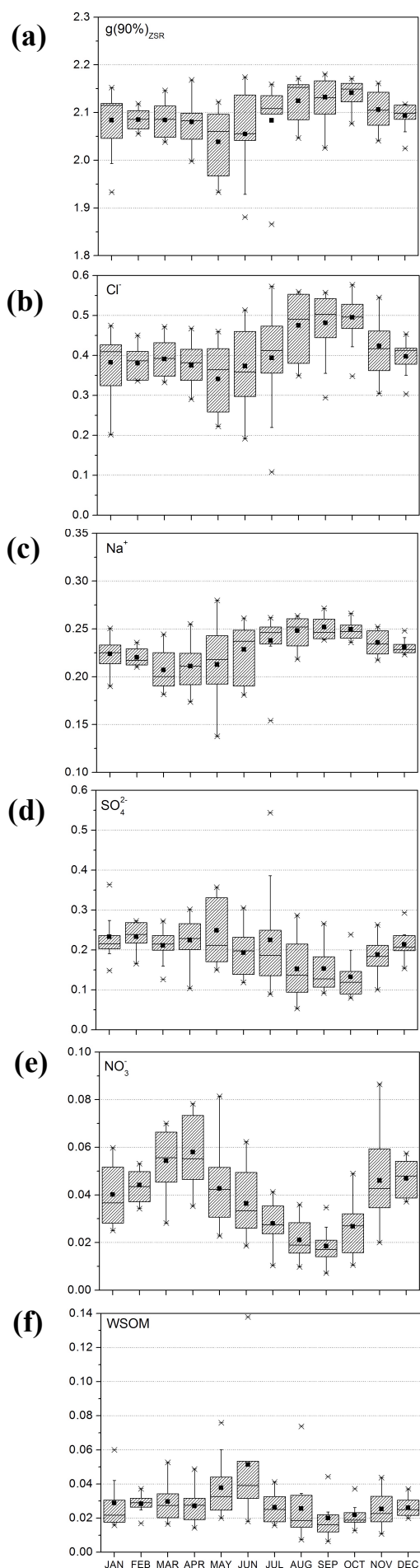


Fig. 3. Box and whisker plot, showing monthly variations in the $g(90\%)_{ZSR}$ and mass fractions of water-soluble matter at Chichijima Island in the western North Pacific during 2001-2012. Mass fractions are calculated using the data of ions and WSOC are taken from Boreddy and Kawamura (2015).

640
 641
 642
 643
 644
 645
 646
 647
 648
 649
 650
 651
 652
 653
 654
 655
 656
 657
 658
 659
 660
 661
 662
 663
 664
 665
 666
 667
 668
 669
 670
 671
 672
 673
 674
 675
 676
 677
 678
 679
 680
 681
 682
 683
 684
 68
 68
 68
 68
 68
 689

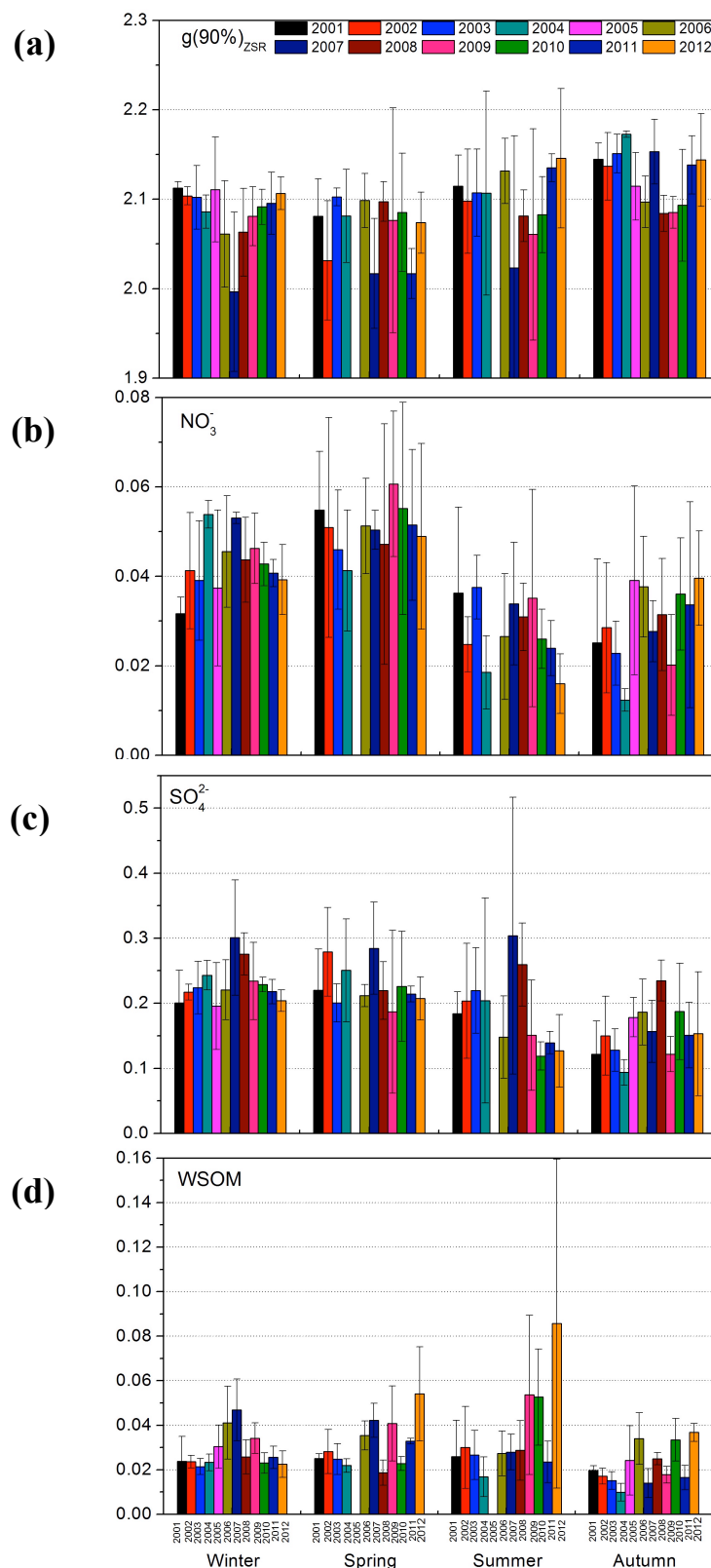


Fig. 4. Annual variations in the $g(90\%)_{ZSR}$ and mass fractions of WSM for different seasons. The data of ions and WSOC are from Boreddy and Kawamura (2015). Mass fractions are calculated using the data of ions and WSOC are taken from Boreddy and Kawamura (2015).

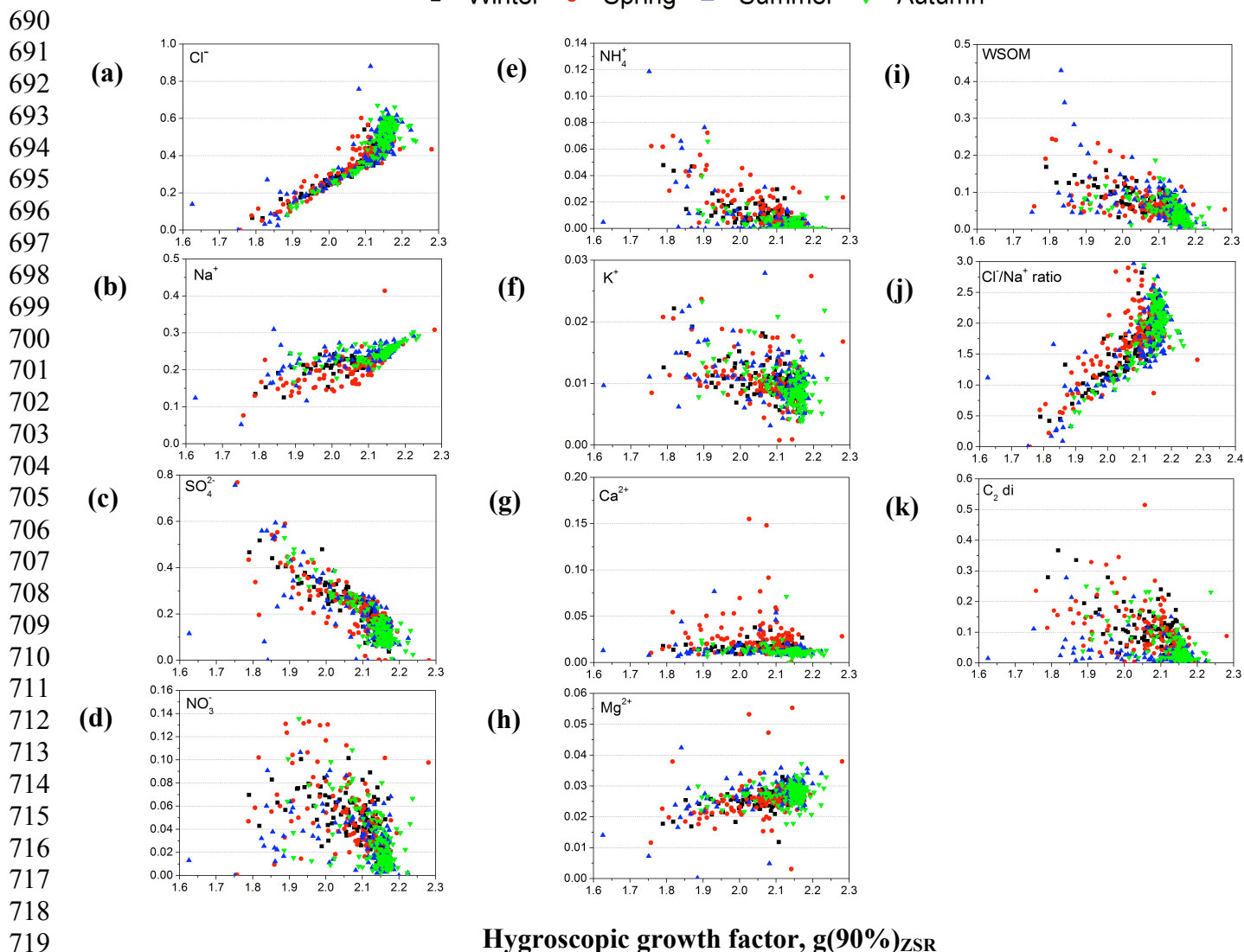


Fig. 5. Scatter plot, showing relation of the $g(90\%)_{\text{ZSR}}$ with (a-i) mass fractions of WSM, (j) Cl^-/Na^+ mass fraction ratio, and (k) $\text{C}_2 \text{ di}$ ($\mu\text{g m}^{-3}$) over the western North Pacific during 2001-2012. Mass fractions are calculated using the data of ions and WSOC are taken from Boreddy and Kawamura (2015).

725
 726

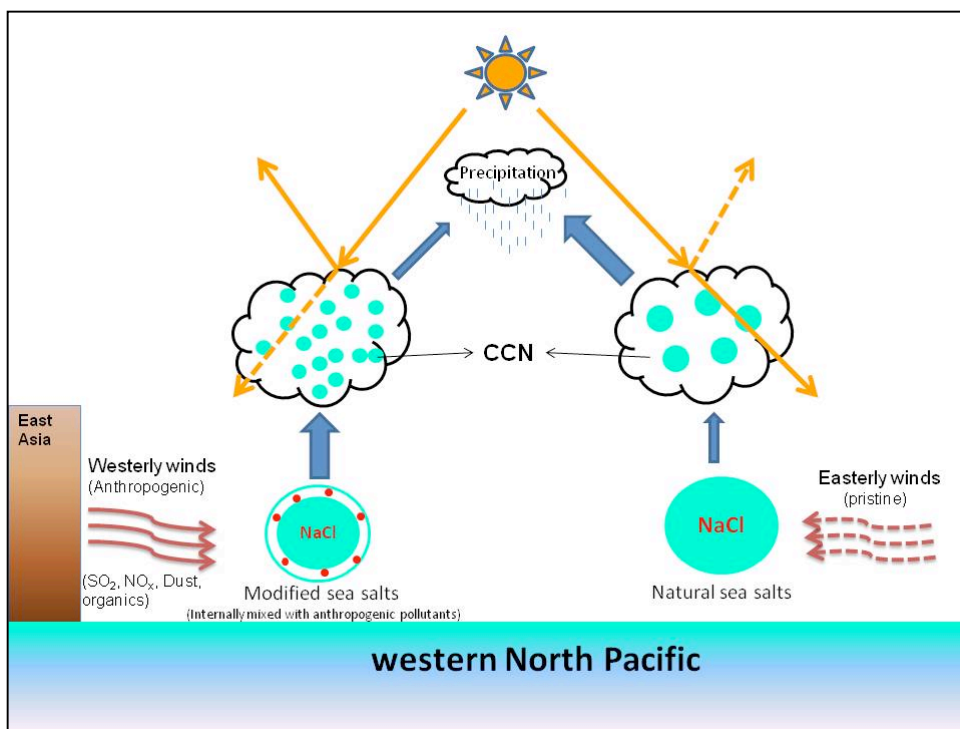


Fig. 6. Schematic diagram, showing changes in physico-chemical properties of sea-salt particles under the influence of two distinct aged air masses over the western North Pacific.

777
778
779
780
781
782
783
784
785
786
787
788
789
790
791
792
793
794
795
796
797
798
799
800
801
802
803
804

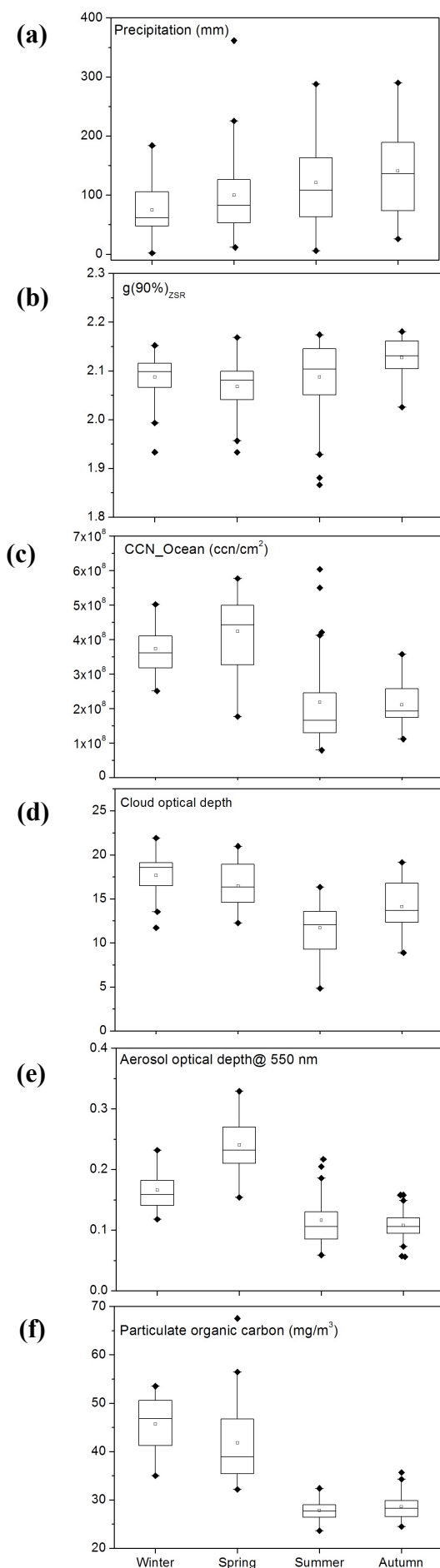


Fig. 7. Box and whisker plots, showing seasonal variations in (a) precipitation, (b) $g(90\%)_{ZSR}$, (c-f) MODIS Aqua satellite products of CCN number concentrations, cloud optical depth, aerosol optical depth, and particulate organic carbon, respectively for the region [140-145°E; 25-30° N] over the western North Pacific during the period of 2001-2012.